RESEARCHERID
THOMSON REUTERS

[Azawi* 4(7): July, 2017] ISSN 2349-4506
Impact Factor: 2.785

Global Journal of Engineering Science and Research Management

MODELING OF BASE ISOLATOR AS STRUCTURAL ELEMENT

Dr. Thamir Al-Azawi*, Dr. AbdulMuttalib I.S. AlMusaui, Dr. Salah R. Al-Zaidee
* Professor of Structural Engineering Department of Civil Engineering, College of Engineering, University of Baghdad, Republic of Iraq
Professor of Structural Engineering Department of Civil Engineering, College of Engineering, University of Baghdad, Republic of Iraq
Lecturer of Structural Engineering Department of Civil Engineering, College of Engineering, University of Baghdad, Republic of Iraq

DOI: 10.5281/zenodo.836621

KEYWORDS: Base Isolation, Modeling of the Base Isolators, Spring Stiffness, Deep Beam Element, Damping

ABSTRACT
Two proposals for modeling of the base isolators as a structural element have been given. The first model simulates base isolator as two springs, while the second one models base isolator as a deep beam element. Comparison between the two models indicates that if the experimental data to determine the value of EI/L are available, the modeling of base isolator as a deep frame element will be more accurate than the model of two springs.

In both models, the energy dissipation in the base isolators has been modeled by an equivalent viscous damping. Based on the comparison with experimental work it is has been found that the equivalent viscous damping can simulate the response of lead - plug rubber bearing with a lower accuracy if compared with modeling the response of low damping rubber bearing. This is mainly due to approximate simulation of inherent nonlinearity nature of lead - plug rubber bearing.

INTRODUCTION
The seismic design should ensure a sufficient strength to sustain the forces induced by a moderate earthquake and sufficient ductility under a strong earthquake. Ductility allows the structure to develop inelastic hinges at beam-ends and column bases during strong motion. These hinges provide not only increased flexibility but also energy–absorbing capacity, both of which help to limit the earthquake generated forces. However, such inelastic deformations require large interstorey displacements and cause progressive breakdown of the structural elements as well as damage to mounted secondary system and non–structural components. Moreover, a structure strengthened to resist an earthquake attack becomes more rigid and larger amplification of the ground acceleration at each floor level may result. Thus, even if the structural member remains in the elastic range under a moderate earthquake, the nonstructural components may be more severely damaged and the danger to occupants may increase (5).

Base isolation is an alternative antiseismic design strategy. In this approach, an isolation system of some kind is used to decouple the superstructure from the ground so that the damaging horizontal component of the earthquake ground motion can be reduced significantly. In general, an isolation system should have sufficient flexibility and energy absorbing capacity. Flexibility in the horizontal direction will lower the fundamental frequency of the structure below the range of frequencies dominating the earthquake input, so that the earthquake–induced loading will be decreased. However, the low stiffness of the isolation system could cause the displacements of the building to become too large. Hence, the isolation system should have some energy–absorbing capacity which, in addition to attenuating the transmission of energy into the building, will also reduce the structural displacements. If the energy–absorbing mechanism involves inelastic behavior, this may be limited to the base isolation system itself and the damage during an earthquake may not be transmitted to the structural members. However, this may cause secondary damage in nonstructural elements (5).

Conventional seismic strengthening design requires adding some structural members, such as shear walls, frames, and bracings. Base isolation may minimize the need for such strengthening members by reducing the earthquake forces imparted to the building. It is therefore an attractive approach for buildings of historical or architectural merit whose appearance and character must be preserved (2).

Despite wide variation in details, base isolations techniques follow two basic approaches with certain common features.

- In the first approach, the isolation system introduces a layer of low lateral stiffness material between the structure and its foundations.
- The second type of isolation system uses rollers or sliders between the foundation and base of the structure.

For a base isolator consisting of a layer of low lateral stiffness the structure will have a natural period of vibration that is much longer than its fixed-base natural period.

As shown in the typical design spectrum of Figure 1 below, the lengthening of period can reduce the pseudo-acceleration and hence the earthquake-induced forces in the structure, but the structural deformations increase across the isolation system.

Conventional seismic strengthening design requires adding some structural members, such as shear walls, frames, and bracings. Base isolation may minimize the need for such strengthening members by reducing the earthquake forces imparted to the building. It is therefore an attractive approach for buildings of historical or architectural merit whose appearance and character must be preserved (2).

This study aims to model the base isolators as structural elements. This was based on the available experimental work from which the stiffness and damping of the base - isolators have been derived. Then Matlab version of Newmark direct integration scheme has been used to solve the resulting linear equation of motion.

The modeling of the following two types of base isolators has been considered in this study:

- Low damping rubber bearing.
- Lead-Plug Rubber Bearing.

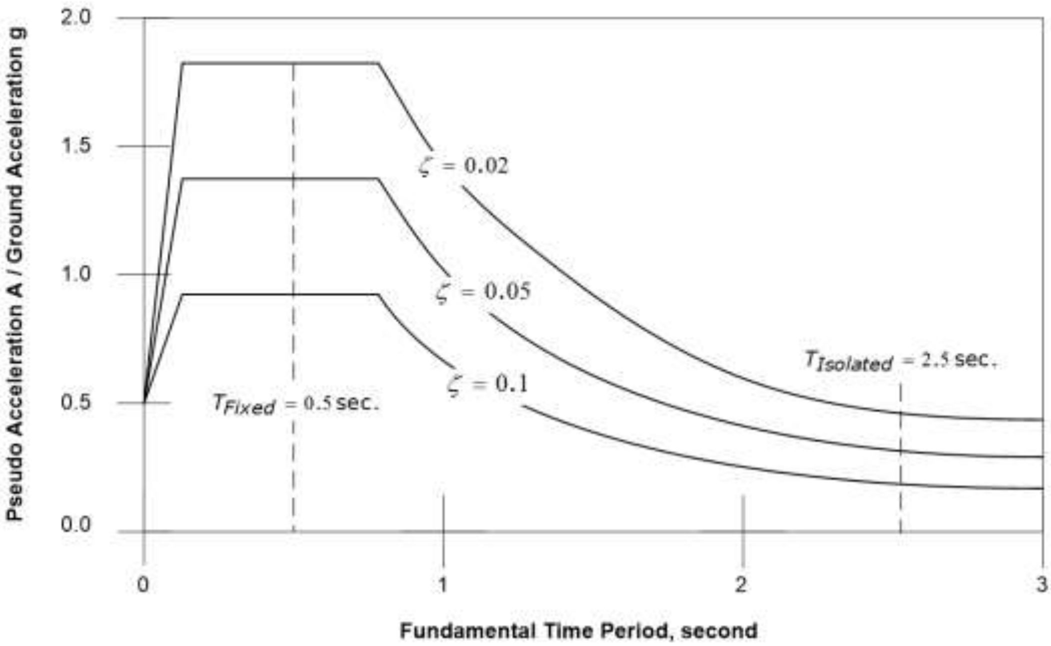

Figure 1: Design spectrum and spectral ordinates for fixed – base and base - isolated systems (2).

BASE ISOLATORS AND THEIR MECHANICAL PROPERTIES

Low – damping natural rubber bearings and synthetic rubber bearings have been widely used in Japan after being strengthened with damping devices such as steel bars, lead bars, or frictional devices. The elastomer used in Japan comprises natural rubber, while in France neoprene has been used in several projects. The isolators have two thick steel endplates and many thin steel shims, as shown in Figure 2. The rubber is vulcanized and bonded to steel in a single operation under heat and pressure in a mold. The steel shims reduce the bulging of rubber and provide a higher vertical stiffness but have little effects on horizontal stiffness, which is controlled by low shear modulus of the elastomer (6).

Figure 2: Low damping rubber bearing.

The bearing behavior in shear is almost linear up to shear strains of (100% to 150%), with a damping ratio in the range of 2-3% of the critical damping (6). Typical relationship between the shear force and the shear displacement for low damping rubber bearing is shown in Figure 3 (4).

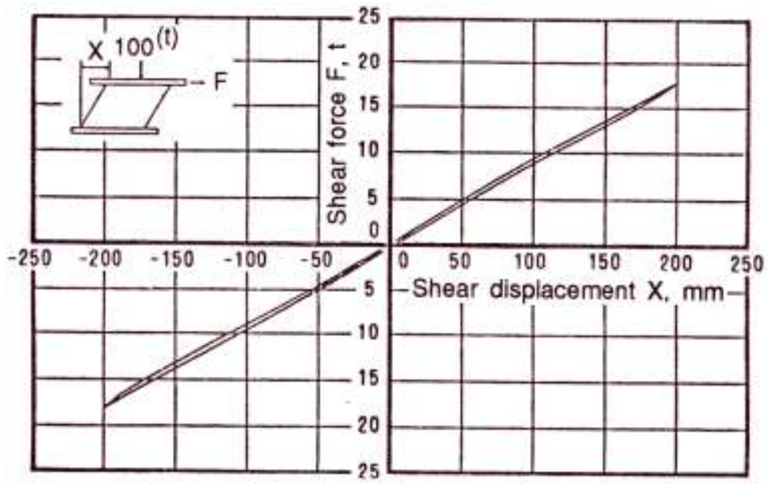

Figure 3: Typical force – displacement relation of low damping rubber bearing.

Roeder and Stanton (9**)** provided a brief description of the state of knowledge with respect to low damping rubber isolators. They stated that, the assumption of bearings behavior as linear, elastic, isotropic and incompressible material (υ=0.5) provides adequate accuracy over the range of applications of this type of base isolator. The correlation between the hardness and the elastic modulus of the elastomer can be derived based on the theory of elasticity for approximate prediction of mechanical properties of bearings. The concept of shape factor, ***S***, (Load Area / Area Free to Bulge) used by design specifications for modeling the relation between the shear stress due to bulging and geometric aspects and reinforcement of bearing had also been discussed.

The advantages of the low damping elastomeric laminated bearings are that; they are simple to be manufactured, easy to model, and their mechanical response is not sensitive to temperature variance, loading history, or aging. The main disadvantage of such bearing is that a supplementary damping system, like the manufacture of linear viscous damper, is generally needed (6).

Lead–plug was invented in New Zealand in 1975 and has been used extensively in New Zealand, Japan, and United States. Lead–plug bearings are laminated rubber bearings similar to low damping rubber bearings but contain one or more lead plugs that are inserted into holes, as shown in Figure 4. The steel plates in the bearing tend to force the lead plug to deform in shear. The lead in the bearing deforms at a shear stress of around 10 MPa, at a bilinear response. It provides, in a single unit, the combined features of vertical load support, horizontal flexibility and energy absorbing capacity required for the base isolation of structures from earthquake attack (6).

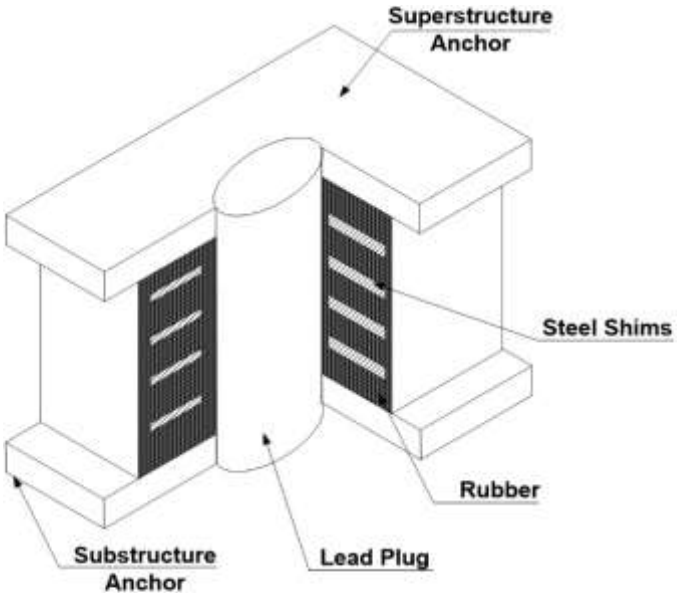

Figure 4: Lead – plug isolators.

Typical relationship between shear force and shear displacement for lead - plug bearing is shown in **Figure 5** (4). **Robinson (**8**)** had made a survey on the testing of the lead – plug bearings. He found that until 1982, a total of eleven bearings had been tested. The main parameters were the bearing diameter (up to 650mm), the lead plug diameter ranging from 50 to 170 mm, the vertical loads (up to 3.15 MN), the stroke (up to), the rates of loading were from 1 mm/h to 100 mm/s, and the temperatures was in range of – 35 ºC to + 45 ºC. In all of these tests, the bearing behaved satisfactorily and the hysteresis loops could be described reasonably well and the lead behaved as an elastic – plastic solid with a yield stress in shear of about 10.5 MPa. The bearings showed little rate dependence at 100 mm/s, though at creep rates of 1mm/h the force in the lead dropped to 30 per cent of that at typical earthquake frequencies. From the tests of six different elastomeric bearings, **Robinson (**8**)** made the following conclusions:

1- The lead – rubber bearing behaves like a bilinear solid with initial elastic shear stiffness, $k_1 \approx 10k_r$where k_r is the post elastic shear stiffness, and with the yield force being determined by the shear stress at which the lead in the bearing yields.
2- The area of the measured hysteresis loop is found to be approximately 80 percent of the loop defined by the bilinear model.

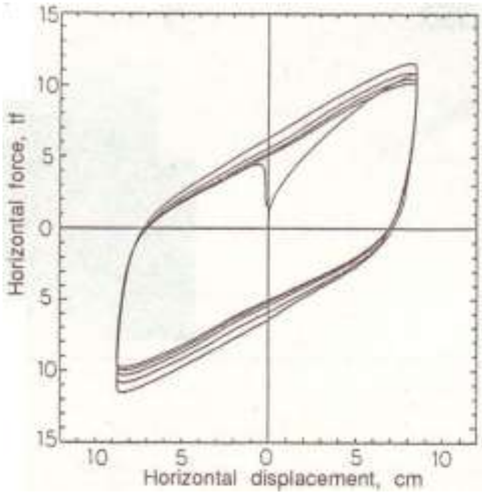

Figure 5: Typical Force – Displacement Relation of Lead - Plug Rubber Bearing (4).

MODELING OF BASE ISOLATORS AS TWO SPRINGS

Due to their objective, the base isolators have large vertical stiffness as compared with the horizontal stiffness. This can lead to model of base isolators as two springs as shown in Figure 6.

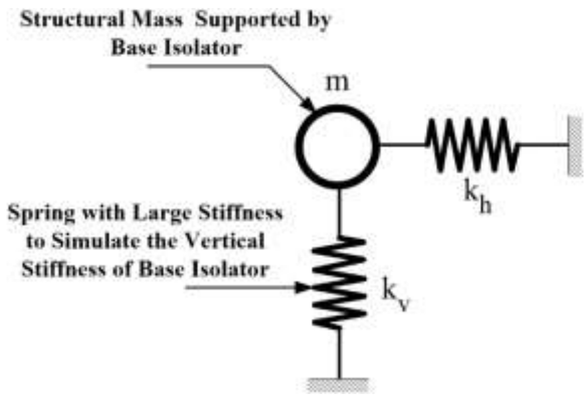

Figure 6: Two-spring model of base isolator.

It is clear that, the two - spring's model can only describe the difference between the vertical and the horizontal stiffnesses of the base isolator and must be modified to be able to describe the energy dissipation mechanisms in the base isolator.

The energy of a vibrating system is dissipated by various mechanisms, and often more than one mechanism may be presented at the same time. It seems difficult to identify or describe mathematically each of these energy dissipating mechanisms in an actual base isolator. As a result, damping in a base isolator is usually represented in a highly idealized manner. For many purposes, the actual damping in a base isolator can be idealized by a linear viscous element or dashpot. The damping coefficient is selected so that the vibration energy dissipated is equivalent to the energy dissipated through all damping mechanisms (2).

The equivalent viscous damper is intended to model the energy dissipation at deformation amplitudes within the linear elastic limit. It is the simplest form of damping to use since the governing differential equation of motion is linear. The advantage of using a linear equation of motion usually outweighs whatever compromises are necessary in the viscous damping approximation (2).

For an actual base isolator, the force-displacement relation obtained from an experiment under cyclic loading with displacement amplitude u_o is determined. Generally, this relation is of arbitrary shape as shown schematically in Figure 7.

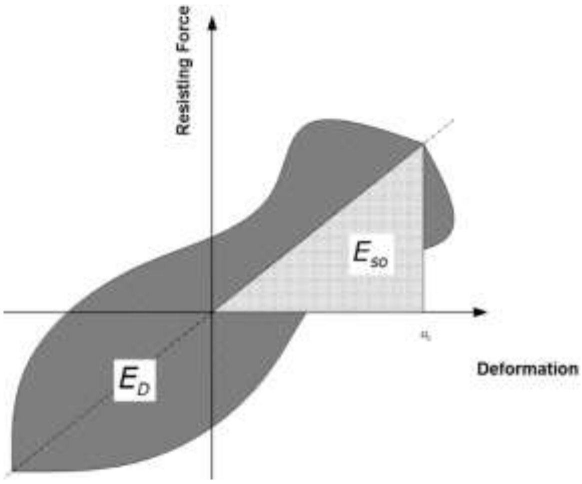

Figure 7: Energy dissipation in a cycle of harmonic vibration determined from experiment on base isolator.

The energy dissipated in the actual base isolator is given by the area ED enclosed by the hysteresis loop. Equating this to the energy dissipated in a viscous damping leads to:

$$\xi_{eq} = \frac{1}{4\pi} \frac{1}{\frac{\omega}{\omega_n}} \frac{E_D}{E_{SO}} \qquad (1)$$

where the strain energy, $E_s = ku_o^2/2$ is calculated from the stiffness k that determined by experiment.
The dissipated energy E_D should be conducted at $= \omega_n$, where the response of the system is most sensitive to damping (2). Thus Eq. (1) specializes to:

$$\xi_{eq} = \frac{1}{4\pi} \frac{E_D}{E_{SO}} \qquad (2)$$

The damping ratio ξ_{eq} is determined from a test at $\omega = \omega_n$ would not be correct at any exciting frequency, but it would be a satisfactory approximation (2).
The above procedure can be applied to low damping rubber bearing that has the force - displacement relation shown in Figure 3 (obtained by test done by (4)) to compute the damping ratio ξ_{eq} for the equivalent viscous damping as follows:

- From the force – displacement relation that shown in Figure 3 compute:
  $k = 875000 \frac{N}{m}$
  $m = 100000\ kg$
  $F = 17.5 \times 10^4 \sin(0.935\ t)$
  then
  $\omega_n = 2.96 \frac{rad}{sec}$.
  And
  $T_n = 2.12\ sec.$
- From ω_n, ω, E_D and Eq.(1), compute
  $\xi_{eq} = 0.02$

The response of the above linear SDF system under the applied harmonic load has been determined by Newmark algorithm. As shown from Figure 8, the viscous damping model can describe the response of low damping rubber bearing with good accuracy.

Additional energy is dissipated in lead-plug rubber base isolator due to inelastic behavior of the lead–plug larger deformations. Under cyclic forces or deformations, this behavior implies formation of a force-deformation hysteresis loop as that shown in Figure 5 (4). This energy dissipation is usually not modeled by viscous damping, especially if the excitation is an earthquake ground motion (2).

Approximate using the equivalent viscous damping model to simulate a lead-plug rubber bearing with force-displacement relation shown in Figure 5, can be summarized as follows:

- From Figure 5 compute the following:
  $k = 1.23 \times 10^6 \frac{N}{m}$
  $m = 85000\ kg$
  $F = 10.5 \times 10^4 \sin(0.628t)$
  Then
  $\omega_n = 3.812 \frac{rad}{sec}$
  and
  $T_n = 1.647\ sec.$
- From ω_n, ω, E_D and Eq.(1), compute $\xi_{eq} = 1.93$

Response of the equivalent linear SDF system that has above parameters is shown in **Figure 9**. From this figure, it is clear that the equivalent viscous damping can simulate the response of lead-plug rubber bearing with lower accuracy if compared with the accuracy of the modeling of the response of low damping rubber bearing. This is mainly due to the approximate modeling of inherent nonlinearity of lead rubber bearing. The more accurate modeling that is based on the bilinear modeling of the lead – plug rubber.

The main disadvantages of the springs modeling is that it cannot simulate the moment at the connection of superstructure with the base isolators.

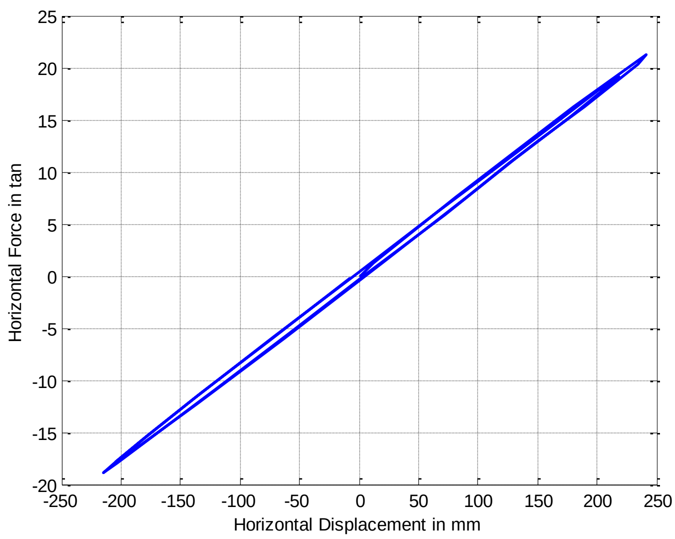

Figure 8: Response of low damping rubber bearing based on equivalent viscous damping model.

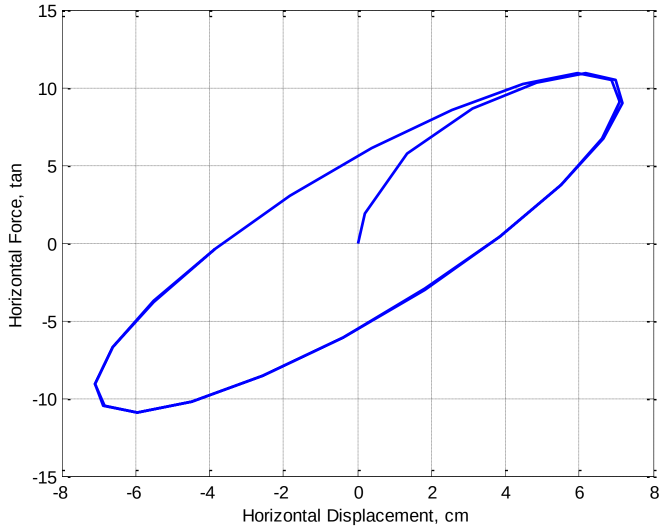

Figure 9: Response of lead-plug rubber bearing based on equivalent viscous damping model.

MODELING OF BASE ISOLATOR AS A DEEP BEAM

Due to its diameter to height ratio, base isolator can be considered as a deep beam element, i.e., the lateral deformation due to shear stress cannot be neglected.

In Timoshenko beam theory, it is assumed that the normal to the neutral axis before deformation remains straight but not necessarily normal to the neutral line after deformation. This implies that the axial displacement $\bar{u}$ at any point (x, z) may be expressed directly in terms of $\theta(x)$ the rotation of the normal so that:

$$\bar{u}(x,z) = z\theta(x) \quad (3)$$

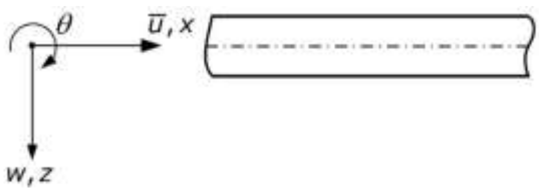

Figure 10. Timoshenko beam coordinates.

It is noted that the normal rotation $\theta(x)$ is equal to the slope of the neutral line dw/dx minus a rotation β which is due to the transverse deformation.

$$\theta(x) = \frac{d\bar{w}}{dx} - \beta \quad (4)$$

Also the lateral (or vertical) displacement $\bar{w}$ at any point (x, z) is given by the lateral displacement at the neutral line so that.

$$\bar{w}(x,z) = w(x) \quad (5)$$

In Timoshenko beam theory, the elastic stress - strain relationships used for unconfined plane stress analysis are usually adopted in a slightly modified form. For convenience it is assumed that the beam is loaded in xz-plane and thus for an isotropic elastic material the relevant stress-strain relationship is

$$\begin{Bmatrix} \sigma_x \\ \tau_{xy} \end{Bmatrix} = \begin{bmatrix} E & 0 \\ 0 & G \end{bmatrix} \begin{Bmatrix} \epsilon_x \\ \gamma_{xz} \end{Bmatrix} \quad (6)$$

where E is Young's modulus and ν is Poisson's ratio. Even if ϵ_x is assumed zero then

$$\sigma_z = 0 \tag{7}$$

as E in z-direction (E_z) is assumed of infinite value (rigid in z-direction). It is possible to write the following stress-strain relationships

$$\sigma_x = E\epsilon_x \text{ and } \tau_{xz} = G\gamma_{xz} \tag{8}$$

where for an isotropic material $G = E/(2(1+\nu))$ is the shear modulus.
The axial strain is given as

$$\epsilon_x = \frac{\partial \bar{u}}{\partial x} = -z\frac{\partial \theta}{\partial x} \tag{9}$$

Similarly, the shear strain γ_{xz} is given as:

$$\gamma_{xz} = \frac{\partial \bar{u}}{\partial y} + \frac{\partial w}{\partial x} = -\theta + \frac{\partial w}{\partial x} = \beta \tag{10}$$

In the analysis of Timoshenko beam element, the lateral displacement w is represented by the relationship (7):

$$w = N_1 w_1 + N_2 w_2 \tag{11}$$

where w_1 and w_2 are the nodal lateral displacements at nodes 1 and 2 and the shape functions (shown in Figure 11) are:

$$N_1 = -\frac{x_2 - x}{L} \qquad N_2 = -\frac{x - x_1}{L} \tag{12}$$

In which x_1 and x_2 are the x-coordinates of local nodes 1 and 2, x is the x-coordinate of a point within the element and L is the length of the element.

Similarly, the normal rotation θ within the element is represented as

$$\theta = N_1\theta_1 + N_2\theta_2 \tag{13}$$

where θ_1 and θ_2 are the normal rotations at local nodes 1 and 2 of the element.

The curvature-displacement relationship can be expressed as

$$\epsilon_f = \begin{bmatrix} 0 & \frac{1}{L} & 0 & -\frac{1}{L} \end{bmatrix} \begin{Bmatrix} w_1 \\ \theta_1 \\ w_2 \\ \theta_2 \end{Bmatrix} = \beta_f \phi \tag{14}$$

where

$$\beta_f = \begin{bmatrix} 0 & \frac{1}{L} & 0 & -\frac{1}{L} \end{bmatrix}$$

is the curvature-displacement matrix and

$$\phi = \begin{Bmatrix} w_1 \\ \theta_1 \\ w_2 \\ \theta_2 \end{Bmatrix}$$

ISSN 2349-4506
Impact Factor: 2.785

Global Journal of Engineering Science and Research Management

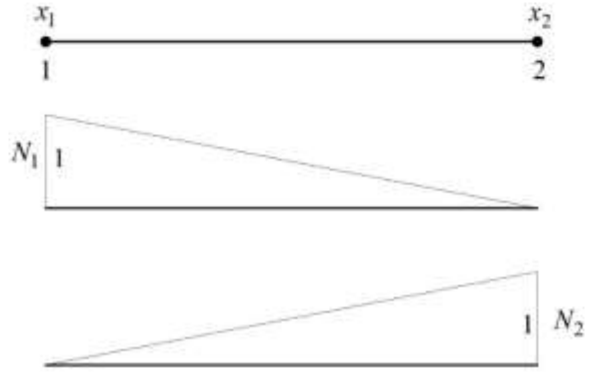

Figure 11: Beam element shape functions.

The shear strain-displacement relationship is given as:

$$\epsilon_s = \left\lfloor -\frac{1}{L} \quad -\frac{x_2 - x}{L} \quad \frac{1}{L} \quad -\frac{(x - x_1)}{L} \right\rfloor \begin{Bmatrix} w_1 \\ \theta_1 \\ w_2 \\ \theta_2 \end{Bmatrix} = \beta_s \phi \qquad (15)$$

where β_s is the Shear Strain-Displacement matrix.

It has been shown that by using a virtual work approach the governing equations can be expressed as (7).

$$\boldsymbol{k} = \boldsymbol{k}_f + \boldsymbol{k}_s \qquad (16)$$

where the submatrices $\boldsymbol{k}_f$ and $\boldsymbol{k}_s$ are

$$\boldsymbol{k}_f = \int_{x_1}^{x_2} \boldsymbol{\beta}_f^T \, EI \, \boldsymbol{\beta}_f \, dx \qquad (17)$$

$$\boldsymbol{k}_s = \int_{x_1}^{x_2} \boldsymbol{\beta}_s^T \, G\hat{A} \, \boldsymbol{\beta}_s \, dx$$

where EI is the flexural rigidity and $G\hat{A}$ is the shear rigidity of the section. The $\hat{A}$ is the effective area of cross section in shear. Usually $G\hat{A} = c^2 GA$ and c^2 is the shear correction factor to transform the nonuniform shear stress in the cross section to uniform shear stress in the cross section.

A deficiency has been pronounced when the element is relatively thin and can cause Shear Locking (1). Therefore, it is possible to find some points at which values of the shear strain represent the average distribution of the shear fields in a particular region (through using a reduced integration scheme) (3).

If one-point Gauss-Legendre reduced integration scheme is used to compute above integrals, the stiffness matrices $\boldsymbol{k}_f$ and $\boldsymbol{k}_s$ will be:

$$\boldsymbol{k}_f = \frac{EI}{L} \begin{bmatrix} 0 & 0 & 0 & 0 \\ 0 & 1 & 0 & -1 \\ 0 & 0 & 0 & 0 \\ 0 & -1 & 0 & 1 \end{bmatrix} \qquad \boldsymbol{k}_s = \frac{G\hat{A}}{L} \begin{bmatrix} 1 & \frac{L}{2} & -1 & \frac{L}{2} \\ \frac{L}{2} & \frac{L^2}{4} & -\frac{L}{2} & \frac{L^2}{4} \\ -1 & -\frac{L}{2} & 1 & -\frac{L}{2} \\ \frac{L}{2} & \frac{L^2}{4} & -\frac{L}{2} & \frac{L^2}{4} \end{bmatrix} \qquad (18)$$

where L is the base isolator length (in the thickness direction) and the ad hoc values of flexural rigidity EI and shear rigidity $G\hat{A}$ can be computed from experimental work (such as that of (4)).

Application of deep beam element model to the low damping rubber bearing leads to the SDF indicated in Figure 12 below.

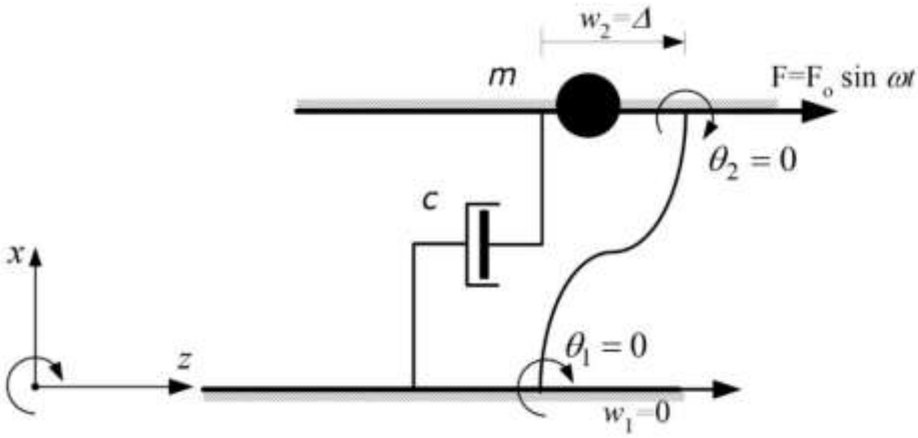

Figurer 12: Deep frame element with viscous damping.

For static analysis

$$\boldsymbol{k}\boldsymbol{\phi} = \boldsymbol{F} \tag{19}$$

where $\boldsymbol{k}$ is the stiffness matrix, $\boldsymbol{\phi}$, is the displacement vector, and $\boldsymbol{F}$ is the force vector.
Substituting the boundary conditions and Eq. (18) into Eq. (19):

$$\frac{EI}{L}\begin{bmatrix} 0 & 0 & 0 & 0 \\ 0 & 1 & 0 & -1 \\ 0 & 0 & 0 & 0 \\ 0 & -1 & 0 & 1 \end{bmatrix}\begin{Bmatrix} 0 \\ 0 \\ \Delta \\ 0 \end{Bmatrix} + \frac{G\hat{A}}{L}\begin{bmatrix} 1 & \frac{L}{2} & -1 & \frac{L}{2} \\ \frac{L}{2} & \frac{L^2}{4} & -\frac{L}{2} & \frac{L^2}{4} \\ -1 & -\frac{L}{2} & 1 & -\frac{L}{2} \\ \frac{L}{2} & \frac{L^2}{4} & -\frac{L}{2} & \frac{L^2}{4} \end{bmatrix}\begin{Bmatrix} 0 \\ 0 \\ \Delta \\ 0 \end{Bmatrix} = \begin{Bmatrix} 0 \\ 0 \\ \mathrm{F} \\ 0 \end{Bmatrix} \tag{20}$$

The solution of the equations gives:

$$\frac{G\hat{A}}{L} = \frac{F}{\Delta} \tag{21}$$

The value of F/Δ can be determined experimentally. For example, for the low damping rubber bearing that has the force-displacement relation shown in Figure 3 can be taken as:

$$\frac{F}{\Delta} = \frac{G\hat{A}}{L} = 875 \times 10^3\ N/m \tag{22}$$

The damping ratio ξ of this SDF can be computed based on equivalent viscous damping concept:

$$\xi = 0.02 \tag{23}$$

From above values of $G\hat{A}/L$ and ξ, it is clear that the resulting SDF system is exactly similar to SDF system that is based on the modeling of base isolator as two springs with viscous damping. Then, the response will be exactly as shown in Figure 8.

In is the same approach, the application of the deep beam model to lead-plug rubber bearing leads to a SDF system similar to that shown in Figure 12 with $G\hat{A}/L = 1.23 \times 10^6\ N/mm$ and $\xi = 1.933$, i.e., to a system that is exactly similar to the system based on modeling of base isolator as two springs with viscous damping. Then the response will be exactly similar to that in Figure 9.

Based on the above interpretations, it seems that modeling of base isolator as a deep beam element and the modeling of a base isolator as two springs are identical. This is generally not true, since if experimental data are available to determine the value of EI/L, the modeling of a base isolator as a deep beam element will be more accurate. In this case, the moment at the connection of superstructure with the base isolator can be simulated.

CONCLUSIONS

From the results of the analysis and comparison with available experimental works, the following conclusions can be drawn:

1. It seems that modeling of the base isolator as a deep beam element and the modeling of the base isolator as two springs are not identical. If experimental data is available to determine the value of EI/L, the modeling of the base isolator as a deep beam element will be more exact and the moment at the connection of superstructure with the base isolator can be simulated.
2. The equivalent viscous damping can simulate the response of lead-plug rubber bearing with lower accuracy if compared with accuracy of modeling the response of low damping rubber bearing. This is mainly due to the approximate modeling of inherent nonlinearity of the lead rubber bearing.

RECOMMENDATIONS

For further work, the following recommendation arises:

1. Assessment of the adequacy of the equivalent viscous damping modeling for base isolators other than the low damping rubber bearing and the lead – plug rubber bearing.
2. Assessment of the adequacy of the bilinear modeling for modeling of the base isolators that are based on sliding.

REFERENCES

1. Bathe, K. J., (1996). Finite Element Procedures. Prentice – Hall International, Inc.
2. Chopra, A. K. (1996). Dynamics of Structures: Theory and Applications to Earthquake Engineering. Prentice-Hall of India, New Delhi.
3. Huang, Hou-Cheng (1988). Static and Dynamic Analysis of Plates and shells: Theory and Applications. Springer Verlag.
4. Japan Building Center, (1993). Technological Development of Earthquake-Resistance Structures. Oxonian Press PVT. LTD., New Delhi.
5. Kelly, J. M. and Tsai, H. C. (1985). Response of Light Internal Equipment in Base
6. Naeim, F. and Kelly, J. M. (1999). Design of Seismic Isolated Structures: From Theory to Practice. John Wily & Sons.
7. Owen, D. R. J., and Hinton, E. (1980). Finite Element in Plasticity: Theory and Practice. Pineridge Press Limited, Swansea, U.K.
8. Robinson, W. H. (1982). Lead – Rubber Hysteretic Bearings Suitable for Protecting Structures During Earthquakes. Journal of Earthquake Engineering and Structural Dynamics, Vol. 10, 593 - 604.
9. Roeder, C. W. and Stanton, J. F. (1983). Elastomeric Bearings: State – of - Art. ASCE, Journal of Structural Engineering, Vol. 109, No. 12.